ORBITAL RESONANCES IN PLANETARY SYSTEMS [1]

Renu Malhotra
Lunar & Planetary Laboratory, The University of Arizona, Tucson, AZ, USA

Keywords. planets, orbits, solar system, Hamiltonian, action-angle variables, perturbation theory, three-body problem, resonance, Kozai-Lidov effect, separatrix, chaos, resonance capture, resonance sweeping, planet migration

Contents

Summary

There are two main types of resonance phenomena in planetary systems involving orbital motions: (i) *mean motion resonance*: This is intuitively the most obvious type of resonance; it occurs when the orbital periods of two planets are close to a ratio of small integers; (ii) *secular resonance*: this is a commensurability of the frequencies of precession of the orientation of orbits, as described by the direction of pericenter and the direction of the orbit normal. It is often possible to identify an unperturbed subsystem and separately a resonant perturbation, which facilitates the use of perturbation theory and other analytical and numerical tools. Resonances can be the source of both stability and instability, and play an important role in shaping the overall orbital distribution

[1]Published in Encyclopedia of Life Support Systems (EOLSS), volume 6.119.55 Celestial Mechanics, Developed under the Auspices of the UNESCO, Eolss Publishers, Paris, France, URL http://www.eolss.net, 2012. *This version corrects errors known to the author as of October 2017.*

and the 'architecture' of planetary systems. This chapter provides an overview of these resonance phenomena, with simple models that elucidate our understanding.

1 Introduction

Consider the simplest planetary system consisting of only one planet, of mass m_1, orbiting a star of mass m_0. Let $\mathbf{r}_0$ and $\mathbf{r_1}$ denote the inertial coordinates of these two bodies. This system has six degrees of freedom, corresponding to the three spatial degrees of freedom for each of the two bodies. Three of these degrees of freedom are made ignorable by identifying them with the free motion of the center-of-mass. The remaining three degrees of freedom can be identified with the coordinates of the planet relative to the star and the problem is reduced to the familiar planetary problem described by the Keplerian Hamiltonian,

$$\mathcal{H}_{\text{kepler}} = \frac{p^2}{2m} - \frac{\mathcal{G}Mm}{r} \tag{1}$$

where $\mathcal{G}$ is the universal constant of gravitation, $\mathbf{r} = \mathbf{r}_1 - \mathbf{r}_0$ is the position vector of the planet relative to the star, $\mathbf{p} = m\dot{\mathbf{r}}$ is the linear momentum of the reduced mass,

$$m = \frac{m_0 m_1}{m_0 + m_1}, \tag{2}$$

and $M = m_0 + m_1$ is the total mass. In this Hamiltonian description, $\mathbf{r}$ and $\mathbf{p}$ are canonically conjugate variables. The general solution of this classic two-body problem is well known in terms of conic sections; the bound solution is called the *Keplerian* ellipse. In this chapter, we will be concerned with only the bound orbits.

The three degrees of freedom for the Kepler system can also be described by three angular variables, one of which measures the motion of the planet in its elliptical orbit and the other two describe the orientation of the orbit in space. The size, shape and orientation of the orbit is fixed in space, and there is only one non-vanishing frequency, namely, the frequency of revolution around the orbit. The orbital elements illustrated in Figure 1 are related to the set of action-angle variables for the two-body problem derived by Charles Delaunay (1816–1872) [see Chapter 1],

$$\begin{aligned} L &= \sqrt{\mathcal{G}Ma}, & \ell &= \text{mean anomaly} \\ G &= \sqrt{\mathcal{G}Ma(1-e^2)}, & \omega &= \text{argument of pericenter}, \\ H &= \sqrt{\mathcal{G}Ma(1-e^2)}\cos i, & \Omega &= \text{longitude of ascending node}, \end{aligned} \tag{3}$$

where a, e and i are the semimajor axis, eccentricity and inclination, respectively, of the bound Keplerian orbit. The mean anomaly, ℓ, is related to the orbital frequency (mean motion), n, which in turn is related to the semimajor axis by Kepler's third law of planetary motion:

$$\dot{\ell} = n = (\mathcal{G}M/a^3)^{\frac{1}{2}}. \tag{4}$$

In equations 3, L, G, H are the action variables and ℓ, ω, Ω are the canonically conjugate angles, known as the *mean anomaly, argument of pericenter* and *longitude of ascending*

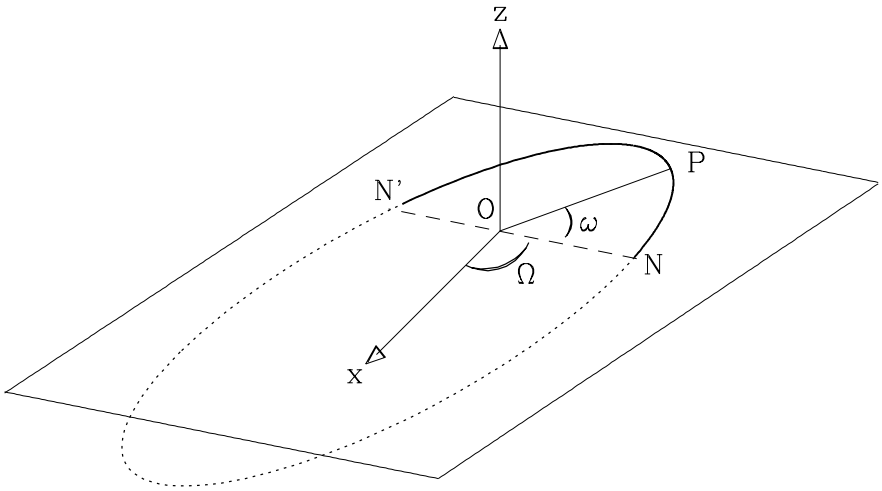

Figure 1: The Keplerian orbit: a planet, m, traces out an ellipse of semimajor axis a and eccentricity e, with the Sun at one focus of the ellipse (which is the origin of the heliocentric coordinate system indicated here). The plane of the orbit has inclination i with respect to the fixed reference plane, and intersects the latter along the line of nodes, NN', where N is the location of the ascending node; the longitude of ascending node, Ω, is the angle from the reference direction x to ON; it is measured in the reference plane. The pericenter is at P; the argument of perihelion ω is the angle from ON to OP; it is measured in the orbital plane. The true anomaly is the instantaneous angular position of the planet measured from OP.

node, respectively. As defined in Eq. (3), the action variables have dimensions of specific angular momentum.

The Kepler Hamiltonian can be expressed in terms of the orbital elements and the Delaunay variables:

$$\mathcal{H}_{\rm kepler} = -\frac{\mathcal{G}Mm}{2a} = -\frac{(\mathcal{G}M)^2 m}{2L^2}. \tag{5}$$

For the case of nearly co-planar and nearly circular orbits, we will also make use of a set of modified Delaunay variables defined by the following canonical set:

$$\begin{aligned} \Lambda &= L, & \lambda &= \ell + \omega + \Omega, \\ \Gamma &= L - G, & \gamma &= -\omega - \Omega \equiv -\varpi, \\ \Upsilon &= L - G - H, & \upsilon &= -\Omega. \end{aligned} \tag{6}$$

For multiple planets around the star, it is desirable to describe the system as a sum of two-body Keplerian Hamiltonians plus the smaller interaction part (the potential energy of the planet-planet interactions). However a similar approach with coordinates relative to the central mass (called 'heliocentric coordinates' in the context of the solar system, more generally 'astrocentric coordinates') does not yield a Hamiltonian that is a sum of two-body Keplerian parts plus an interaction part, as we might naively expect. This is because the kinetic energy is not a diagonal sum of the squares of the momenta

in relative coordinates. This problem is overcome by using a special coordinate system invented by Carl Jacobi (1804–1851), in which we use the coordinates of the center-of-mass, and then, successively, the coordinates of the first planet relative to the star, the coordinates of the second planet relative to the center-of-mass of the star and the first planet, and so on. For a system of N planets orbiting a star, let $\mathbf{r}_i (i = 0, 1, ...N)$ denote the coordinates of the star and the N planets in an inertial reference frame; then the Jacobi coordinates are given by

$$\tilde{\mathbf{r}}_0 = \frac{\sum_{j=0}^{N} m_j \mathbf{r}_j}{\sum_{j=0}^{N} m_j}; \qquad \tilde{\mathbf{r}}_i = \mathbf{r}_i - \mathbf{R}_{i-1}, \qquad \text{with } \mathbf{R}_i = \frac{\sum_{j=0}^{i} m_j \mathbf{r}_j}{\sum_{j=0}^{i} m_j}, \tag{7}$$

and the conjugate momenta,

$$\tilde{\mathbf{p}}_i = \tilde{m}_i \dot{\tilde{\mathbf{r}}}_i, \qquad \text{with } \tilde{m}_i = \frac{m_i \sum_{j=0}^{i-1} m_j}{\sum_{j=0}^{i} m_j}. \tag{8}$$

Then the Hamiltonian for the N–planet system is given by

$$\mathcal{H} = \frac{\tilde{p}_0^2}{2\sum_{j=0}^{N} m_j} + \sum_{i=1}^{N} \frac{\tilde{p}_i^2}{2\tilde{m}_i} - \sum_{i=1}^{N} \frac{G m_0 m_i}{r_{i0}} - \sum_{0<i<j} \frac{G m_i m_j}{r_{ij}}, \tag{9}$$

and r_{i0} is the distance between the star and the i^{th} planet, and r_{ij} is the distance between planet i and planet j. Because r_{i0} and r_{ij} do not depend upon the center-of-mass position, this Hamiltonian is independent of $\tilde{\mathbf{r}}_0$, and it follows that $\tilde{\mathbf{p}}_0$ is a constant. Thus, the first term in Eq. (9), which is the center-of-mass kinetic energy, is a constant. By construction, the remaining kinetic energy terms are a diagonal sum of the squares of the new momenta. We can now obtain a Hamiltonian which is a sum of N unperturbed Keplerian Hamiltonians and a small perturbation:

$$\mathcal{H} = \sum_{i=1}^{N} \Big[\frac{\tilde{p}_i^2}{2\tilde{m}_i} - \frac{G m_0 m_i}{\tilde{r}_i} \Big] - \sum_{0<i<j} \frac{G m_i m_j}{r_{ij}} + \sum_{i=1}^{N} \Big[\frac{G m_0 m_i}{\tilde{r}_i} - \frac{G m_0 m_i}{r_{i0}} \Big]. \tag{10}$$

In deriving Eq. (10) from Eq. (9), we omitted the constant center-of-mass kinetic energy term and we added and subtracted $\sum_{i=1}^{N} G m_0 m_i / \tilde{r}_i$. In Eq. (10), we can recognize the first series as a sum of N independent Keplerian Hamiltonians. The second series describes the direct planet-planet interactions. The last series consists of terms that are differences of two large quantities; these difference terms are each of order $\sim m_i m_j$, i.e., of the same order as the terms in the direct planet-planet interactions, and is referred to as the 'indirect' perturbation. Thus, the Hamiltonian of Eq. (10) is of the form

$$\mathcal{H} = \sum_{i=1}^{N} \mathcal{H}_{\text{kepler}}^{(i)} + \mathcal{H}_{\text{interaction}}, \tag{11}$$

which is suitable for the tools of perturbation theory.

An important special case of the perturbed system is when one of the bodies is of infinitesimal mass, a 'test particle'. The test particle does not affect the massive bodies but is perturbed by them. Let the unperturbed orbit of the test particle be a Keplerian ellipse about m_0. Then the specific energy of the test particle can be written as a sum of its unperturbed Keplerian Hamiltonian, $\mathcal{H}_{\rm testparticle} = -\mathcal{G}m_0/2a$, and an interaction part owing to the perturbations from N planets,

$$\mathcal{H}_{\rm tp,interaction} = -\sum_{j=1}^{N} \mathcal{G}m_j \left[\frac{1}{|\mathbf{r}_{\rm tp} - \mathbf{r}_j|} - \frac{(\mathbf{r}_{\rm tp} - \mathbf{r}_0)\cdot(\mathbf{r}_j - \mathbf{r}_0)}{|\mathbf{r}_j - \mathbf{r}_0|^3} \right]. \tag{12}$$

The perturbations, $\mathcal{H}_{\rm interaction}$, cause changes in the Keplerian orbital parameters. The Delaunay variables are of course no longer action-angle variables, but they provide a useful canonical set; we will make use of it in the following sections. Qualitatively, the perturbed Keplerian orbit gains two slow frequencies, the precession of the direction of pericenter and the precession of the line of nodes (equivalently, the pole) of the orbit plane; these are slow relative to the mean motion, n.

Resonance

A *secular resonance* involves a commensurability amongst the slow frequencies of orbital precession, whereas a *mean motion resonance* is a commensurability of the frequencies of orbital revolution. The timescales for secular perturbations are usually significantly longer than for [low order] mean motion resonant perturbations, but there is also a coupling between the two which leads to resonance splittings and chaotic dynamics. The boundaries (or separatrices) of mean motion resonances are often the sites for such interactions amongst secular and mean motion resonances.

A mean motion resonance between two planets occurs when the ratio of their mean motions or orbital frequencies n_1, n_2 is close to a ratio of small integers, $(p+q)/p$ where $p \neq 0$ and $q \geq 0$ are integers. The case $q = 0$ is sometimes called a corotation or co-orbital resonance; a prominent example in the solar system is the Trojan asteroids which share the mean motion of Jupiter but librate approximately $\pm 60^\circ$ from Jupiter's mean longitude. When $q > 0$, it is called the order of the resonance; this is because the strength of the resonant potential is proportional to e^q or i^q when the eccentricities e and inclinations i of the planets are small. Inclination resonances occur only for even values of q. In a resonant configuration, the longitude of the planets at every q^{th} conjunction librates slowly about a direction determined by the lines of apsides and nodes of the planetary orbits. In terms of the action-angle variables for the Keplerian Hamiltonian, this geometry is naturally described by the libration of a so-called *resonant angle* which is a linear combination of the angular variables. For example, for the 2:1 mean motion resonance between a pair of planets, two possible resonant angles are

$$\phi_1 = 2\lambda_2 - \lambda_1 - \varpi_1, \qquad \phi_2 = 2\lambda_2 - \lambda_1 - \varpi_2. \tag{13}$$

Close to the 2:1 mean motion resonance, both these angles have very slow variation (slow in comparison with the mean motions). The planet pair is said to be *in resonance* if at

least one resonant angle exhibits a libration; in this case, the long term average rate of the resonant angle vanishes, and we speak instead of its 'libration frequency'. If a resonant angle does not librate but rather varies over the entire range 0 to 2π cyclically, we speak of its 'circulation frequency'.

How close does the mean motion ratio need to be for a planet pair to be considered resonant? There is not a precise answer to this question. A rough answer is provided by an estimate of the range, Δn, of orbital mean motion over which it is possible for the resonant angle to librate. For nearly circular orbits, and for $0 \leq q \leq 2$, this estimate is given by

$$\frac{\Delta n}{n} \simeq \mu^{\frac{q+1}{3}} \tag{14}$$

where μ is the planet-Sun mass ratio.

Amongst the major planets of the solar system, no planet pair exhibits a resonant angle libration, although several are close to resonance: Jupiter and Saturn are within 1% of a 5:2 resonance, Saturn and Uranus are within 5% of a 3:1 resonance, and Uranus and Neptune are within 2% of a 2:1 resonance. In the first extra-solar planetary system to be discovered, the three-planet system PSR B1257+12, the outer two planets are within 2% of a 3:2 resonance. None of these is close enough to exact resonance to exhibit a resonant angle libration. Amongst the several hundred extra-solar multiple planet systems detected by the *Kepler* space mission recently, it is estimated that at least $\sim 30\%$ harbor near-resonant pairs. One extra-solar planetary system, GJ 876, with four planets, appears to have at least two pairwise 2:1 resonances close enough to be in libration. In some of these cases, the nearness to resonance causes orbital perturbations large enough to be detectable, and has allowed measurements of the planetary masses and orbital inclinations.

Somewhat in contrast with the planets, several pairs of satellites of the solar system's giant planets exhibit librations of resonant angles; these include the Galilean satellites Io, Europa and Ganymede of Jupiter, and the Saturnian satellite pairs Janus and Epimetheus, Mima and Tethys, Enceladus and Dione, Titan and Hyperion. The existence of these near-exact commensurabilities, as evidenced by the librating resonant angles, in the satellite systems has been a subject of much study over the past few decades. These are now generally understood to be the consequence of very small dissipative effects which alter the orbital semimajor axes sufficiently over very long timescales so much so that initially well separated non-resonant orbits evolve into an exact resonance state characterized by a librating resonant angle. Once a resonant libration is established, it is generally stable to further adiabatic changes in the individual orbits due to continuing dissipative effects. This hypothesis provides a plausible explanation for the most prominent cases of mean motion resonances amongst the Jovian and Saturnian satellites. However, the Uranian satellites present a challenge to this view, as there are no exact resonances in this satellite system, and it is unsatisfactory to argue that somehow tidal dissipation is vastly different in this system. An interesting resolution to this puzzle was achieved when the dynamics of orbital resonances was analyzed carefully and the role

of the small but significant splitting of mean motion resonances and the interaction of neighboring resonances was recognized. Such interactions can destabilize a previously established resonance, so that mean motion resonance lifetimes can be much shorter than the age of the solar system. Studies of the Jovian satellites, Io, Europa and Ganymede, also suggest a dynamic, evolving resonant orbital configuration over the history of the solar system.

Another notable example of resonance in the solar system is the dwarf planet Pluto whose orbit is resonant with the planet Neptune, and exhibits a libration of a 3:2 resonant angle; the origin of this mean motion commensurability is now understood to be owed to the orbital migration of Neptune driven by interactions with the disk of planetesimals left over from the planet formation era. Studies of this mechanism have led to new insights into the early orbital migration history of the solar system's giant planets, and it is a very active area of current research.

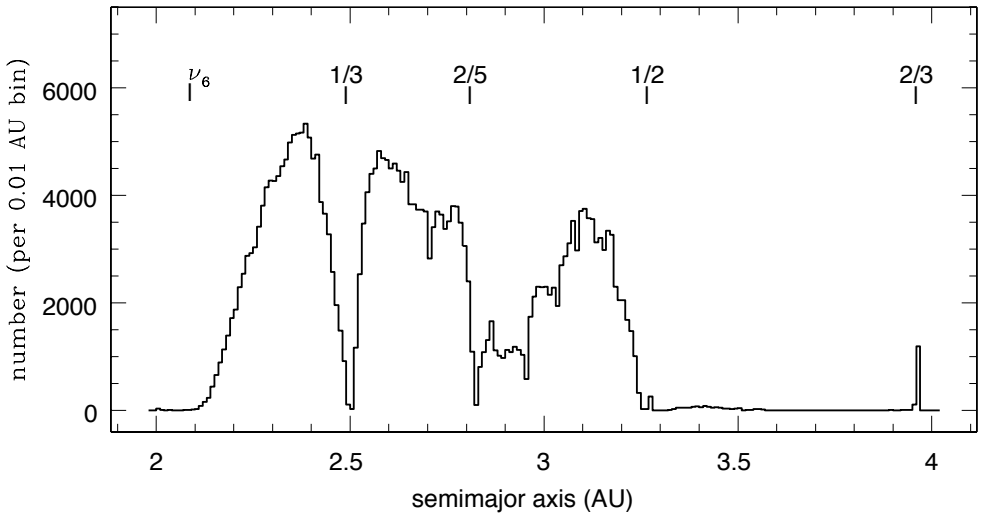

Figure 2: The semimajor axis distribution of asteroids in the main asteroid belt. The locations of several resonances are indicated near the top. (Data for all numbered asteroids from http:hamilton.dm.unipi.it/astdys/; synthetic proper elements computed numerically.)

The population of minor planets in the main asteroid belt in the solar system offers one of the most well-studied examples of the role of orbital resonances in shaping the distribution of orbits. Figure 2 plots the distribution of semimajor axis of asteroids in the main asteroid belt. (Note that some of the non-uniformities in the number distribution are attributable to observational selection effects: astronomical surveys for faint bodies in the solar system remain quite incomplete, so that many smaller and more distant objects remain undiscovered.) The inner edge of the asteroid belt is defined by a secular resonance, known as the ν_6 secular resonance, in which the apsidal secular precession rate of an asteroid is nearly equal to the apsidal precession rate of Saturn. There are

several prominent deficits coinciding with the locations of mean motion resonances with Jupiter; this correlation was first noted by Daniel Kirkwood (1814–1895) and the deficits are known as the Kirkwood Gaps. Interestingly, these gaps are significantly wider than would be anticipated by simple estimates of the resonant widths, such as in Eq. (14). Deeper analyses have revealed that chaotic dynamics owed to the small secular variations of the orbit of Jupiter are very important in widening the Kirkwood gaps, and, beyond that, even the early orbital migration history of Jupiter and Saturn is recorded in the widths and shapes of these gaps.

There also exist orbital resonances that do not neatly fall into the categories of 'mean motion resonance' or 'secular resonance'. For example, the angular velocity of the apsidal precession rate of a ringlet within the C-ring of Saturn is commensurate with the orbital mean motion of Titan, the so-called Titan 1:0 apsidal resonance. Two retrograde moons of Jupiter, Pasiphae and Sinope, exhibit a 1:1 commensurability of their perijove apsidal precession rate with Jupiter's heliocentric apsidal precession rate. So-called three-body resonances which involve a sequence of commensurable mean motions of a test particle with two planets have been identified as a source of weak chaos and orbital instability on giga year timescales; these may explain the absence of asteroids in some regions of the solar system that otherwise appear to be stable. A class of resonances known as 'super resonances' or 'secondary resonances' have been identified in the very long term evolution of planetary and satellite orbits; these are defined by small integer ratio commensurabilities between the libration frequency of a resonant angle and the circulation frequency of a different resonant angle. Pluto's orbit and the Uranian satellite system provide two well-studied examples of this type of resonance.

2 Secular resonances

2.1 Kozai-Lidov effect

One of the most surprising and non-intuitive resonances in the so-called restricted three-body problem was identified in 1962 by two authors, Y. Kozai (1928–) and M. Lidov (1949–), working independently and on two quite different problems. The former author was interested in the long term orbital evolution of highly inclined asteroid orbits perturbed by Jupiter, while the latter author was studying the orbits of geocentric artificial satellites under lunar, solar and other perturbations. The surprising result they found was an instability of circular orbits of high inclination. This section provides a simplified analysis of what is now called the Kozai-Lidov effect. This is a type of secular resonance in which the apsidal and nodal precession rates are equal and of opposite sign, and the orbital eccentricity is excited from small to large values on secular timescales. This effect has been invoked more recently in several astrophysical contexts: to understand the short merger timescales of compact objects, to explain the orbital distribution of binary stars, and to explain several surprising features of exo-planetary systems, such as the presence of so-called 'hot Jupiters' (jovian mass gaseous giant planets in very tight orbit about

their stars), large stellar obliquities to the orbital planes of hot Jupiters, and high orbital eccentricities of many exo-planets.

Consider a test particle in orbit about a star of mass m_* (semi-major axis a and eccentricity e) subject to perturbation by a distant planet $m_{\rm p}$ which also orbits m_* in a circular orbit of radius $a_{\rm p}$. This is one of the simplest of the special cases described by Eq. (12). The interaction potential in this case can be written as

$$\mathcal{H}_{\rm tp,interaction} = -\mathcal{G}m_{\rm p}\left[\frac{1}{|\mathbf{r}_{\rm tp}-\mathbf{r}_{\rm p}|} - \frac{\mathbf{r}_{\rm tp}\cdot\mathbf{r}_{\rm p}}{r_{\rm p}^3}\right] \tag{15}$$

where $\mathbf{r}_{\rm tp}, \mathbf{r}_{\rm p}$ now denote the astrocentric coordinates of the test particle and the planet, respectively. We wish to determine the changes in the shape and orientation of the particle's orbit on timescales long compared to the orbital periods. To do this for $r_{\rm p} \gg r_{\rm tp}$, we expand the interaction potential in powers of $r_{\rm tp}/r_{\rm p}$, retaining terms to second order, and we then average the perturbation potential over the orbital period of the perturber as well as over the orbital period of the test particle. After some tedious algebra, the perturbation potential averaged over the mean longitudes of both the planet and the test particle can be expressed in terms of orbital elements:

$$\langle\mathcal{H}_{\rm tp,interaction}\rangle \simeq -\frac{\mathcal{G}m_{\rm p}a^2}{8a_{\rm p}^3}[2+3e^2-3(1-e^2+5e^2\sin^2\omega)\sin^2 i]. \tag{16}$$

Here we have omitted an inessential constant, $-\mathcal{G}m_{\rm p}/a_{\rm p}$, and we have adopted the planet's fixed orbit plane as the reference plane, so the test particle's orbit inclination, i, is relative to the planet's orbit plane, and its argument of periastron, ω, is measured from the ascending node on that reference plane; a and e are the semimajor axis and eccentricity of the test particle's orbit.

The averaged interaction Hamiltonian is independent of ℓ and Ω, therefore L and H are constants of the perturbed motion, but G is not. However, $\langle\mathcal{H}_{\rm tp,interaction}\rangle$ is time-independent and is therefore also a constant of the motion. Thus, with three independent constants of motion for the 3-degree-of-freedom system, the problem is completely integrable. We can use these to describe the behavior of the solutions.

From the first integrals L and H, it follows that the particle's semimajor axis, a, is constant, as well as

$$\Theta_1 \equiv \sqrt{1-e^2}\cos i = \text{constant}. \tag{17}$$

Θ_1 is sometimes called the Kozai integral. Furthermore, from the condition $\langle\mathcal{H}_{\rm tp,interaction}\rangle =$ constant, it follows that

$$\Theta_2 \equiv e^2(2-5\sin^2\omega\sin^2 i) = \text{constant}. \tag{18}$$

Because the Hamiltonian does not depend upon Ω, the phase space trajectories can be represented on the G–ω plane alone, as the level curves of $\langle\mathcal{H}_{\rm tp,interaction}\rangle$. Moreover, since L is a constant, the phase space structure is the same for any value of the semimajor

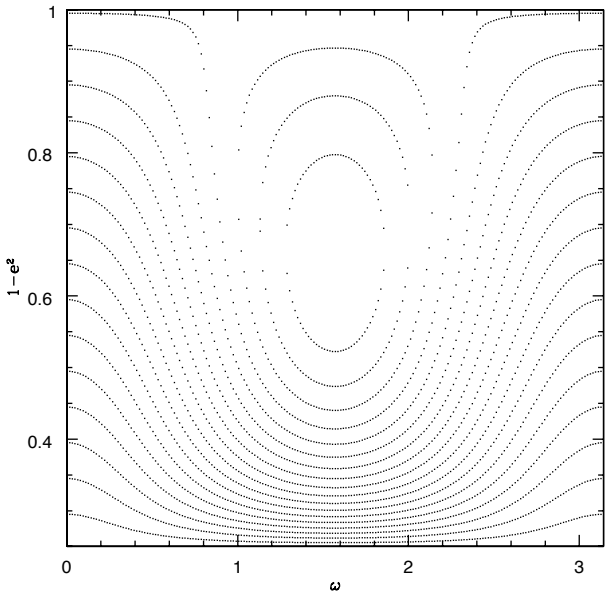

Figure 3: Level curves of $\langle \mathcal{H}_{tp,interaction} \rangle$, for $\Theta_1 = 0.5$.

axis a (within the quadrupole approximation) and can be represented on the $(\sqrt{1-e^2}, \omega)$ plane. An example is shown in Figure 3. We see that there is a region of the phase space where the argument of pericenter, ω, is in libration. At the center of the libration zone ω is stationary. Physically, this corresponds to the state in which the precession rate of the line of nodes is equal in magnitude but opposite in sign to the precession rate of the longitude of pericenter.

To obtain the equations of motion, it is helpful to write $\langle \mathcal{H}_{\rm tp,interaction} \rangle$ in terms of the canonical Delaunay variables:

$$\langle \mathcal{H}_{\rm tp,interaction} \rangle = -\frac{\mathcal{G} m_{\rm p} a^2}{8 a_{\rm p}^3} \left[5 + 3\frac{H^2}{L^2} - 6\frac{G^2}{L^2} - 15\Big(1 - \frac{G^2}{L^2} - \frac{H^2}{G^2} + \frac{H^2}{L^2}\Big) \sin^2\omega \right]. \quad (19)$$

Then Hamilton's equations yield:

$$\dot{\Omega} = \frac{\partial \mathcal{H}}{\partial H} = -\frac{3\mathcal{G} m_p a^2}{4 a_{\rm p}^3} \frac{H}{L^2} \left[1 - 5\Big(1 - \frac{L^2}{G^2}\Big) \sin^2\omega \right], \quad (20)$$

$$\dot{\omega} = \frac{\partial \mathcal{H}}{\partial G} = \frac{3\mathcal{G} m_p a^2}{4 a_{\rm p}^3 G} \left[2\frac{G^2}{L^2} + 5\Big(\frac{H^2}{G^2} - \frac{G^2}{L^2}\Big) \sin^2\omega \right], \quad (21)$$

$$\dot{G} = -\frac{\partial \mathcal{H}}{\partial \omega} = -15 \frac{\mathcal{G} m_p a^2}{8 a_{\rm p}^3} e^2 \sin^2 i \sin 2\omega. \quad (22)$$

The stationary solutions are obtained by demanding $\dot{\Omega} = 0$, $\dot{\omega} = 0$ and $\dot{G} = 0$. By inspection of Eq. (22), we see that $\dot{G} = 0$ whenever $\omega = 0, \pm\frac{1}{2}\pi, \pi$.

At $\omega = 0, \pi$, $\dot{\omega}$ vanishes for $G = 0$, i.e., $e = 1$.

At $\omega = \pm\frac{1}{2}\pi$, $\dot{\omega}$ vanishes for $G = (5H^2L^2/3)^{1/4}$, i.e., $e^2 = 1 - (5\Theta_1^2/3)^{\frac{1}{2}}$, $\cos^2 i = (3\Theta_1/5)^{\frac{1}{2}}$. Note that these are physical solutions only for $\Theta_1^2 \leq \frac{3}{5}$.

It is interesting to consider the case of small e, large i:

$$\dot{G} = -\frac{Ge\dot{e}}{1-e^2} = -15\frac{\mathcal{G}m_{\rm p}a^2}{8a_{\rm p}^3}e^2\sin^2 i\sin 2\omega \tag{23}$$

or

$$\frac{\dot{e}}{e} \simeq \frac{15m_{\rm p}a^3}{8m_*a_{\rm p}^3}n\sin^2 i\sin 2\omega \tag{24}$$

We see that, for small e, the eccentricity grows exponentially. This is the reason why the Kozai-Lidov effect is also sometimes referred to as the 'Kozai resonance' (in analogy with a resonantly forced oscillator whose amplitude grows without bound). The characteristic growth timescale of the eccentricity is

$$T_{\rm K\text{-}L} = \left[\frac{15m_{\rm p}a^3}{8m_*a_{\rm p}^3}n\right]^{-1}. \tag{25}$$

Examples

$$T_{\rm K-L} \simeq \left\{ \begin{array}{ll} 530(R_\oplus/a)^{\frac{3}{2}}{\rm yr} & \text{solar perturbation on earth satellite} \\ 70(R_\oplus/a)^{\frac{3}{2}}{\rm yr} & \text{lunar perturbation on earth satellite} \\ 1.3(R_{\rm moon}/a)^{\frac{3}{2}}{\rm yr} & \text{earth perturbation on lunar satellite} \end{array} \right\} \tag{26}$$

where $R_\oplus, R_{\rm moon}$ are the radius of the planet Earth and of the moon, respectively.

The eccentricity growth is actually not unbounded, rather it is bounded by the constraints set by the first integrals, Eq. (17)–(18). For initially $\sim$zero eccentricity, the maximum eccentricity is achieved at $\omega = \pm\frac{1}{2}\pi$ and $\cos^2 i = \frac{3}{5}$, so that $e^2_{\rm max} = 1 - \frac{5}{3}\cos^2 i_0$, where i_0 is the initial inclination. From the latter condition, we see that the eccentricity growth will occur for $\cos^2 i_0 < \frac{3}{5}$, i.e., $i_1 < i_0 < i_2$, where $i_1 = \arccos\sqrt{\frac{3}{5}} \simeq 0.685$ ($\sim 39^\circ.2$), and $i_2 = \pi - i_1$. That is, circular test particle orbits are unstable and undergo exponential eccentricity growth if they are inclined greater than $\sim 39^\circ$ and less than $\sim 141^\circ$ with respect to the distant planet's orbit plane.

In the case of polar satellites of Earth, the large oblateness of the Earth's figure causes a significant precession of apsides and nodes; this effectively kills the Kozai-Lidov instability of geocentric polar orbits, hence allowing the happy fact of many man-made polar satellites to have long stability times.

Finally, we mention some interesting new research regarding the Kozai-Lidov effect. Note that the preservation of the Kozai integral, Eq. (17), implies that the sign of $\cos i$ cannot change, i.e., a prograde orbit ($0 \leq i \leq 90^\circ$) remains prograde and a retrograde orbit ($90^\circ \leq i \leq 180^\circ$) remains retrograde, so that 'flipping' of the orbital plane is not allowed. However, this is true only in the second-order (quadrupole) truncation of the interaction Hamiltonian, Eq. (16). It has recently been pointed out that the higher order perturbations induce time variability of the Kozai integral; for sufficiently strong octupole perturbations, even orbit 'flips' can occur albeit on very long timescales.

2.2 Linear secular resonance

A different case of secular resonance occurs for a test particle perturbed by a planetary system of nearly coplanar, nearly circular planetary orbits. For example, at specific locations, i.e., narrow range of semimajor axis values, a test particle's initially circular orbit can be excited to high eccentricity —eventually even becoming parabolic— by means of slow forcing by the secular variations of the planets. This phenomenon is thought to be responsible for a class of 'Sun-grazing' comets discovered by the solar space probe SOHO; these objects likely originate in the asteroid belt and are subjected to an eccentricity secular resonance which changes their initial low eccentricity orbits into high eccentricity orbits having perihelion distance near the solar surface. This type of resonance is also important in explaining a prominent gap found in the Kuiper belt. In the early history of the solar system, this type of resonance is thought to have been very important in the dynamical transport of asteroids and comets and in the excitation of planetesimal orbits during planet formation processes.

This classic linear resonance phenomenon is most simply illustrated with a model of a test particle orbiting a star, and perturbed by N planets, all in low eccentricity, low inclination orbits. Since the test particle does not perturb the motion of the planets, let us first consider the perturbed motion of the planets.

Secular perturbation theory for planets

Assuming that the planets are not near any mean motion resonance, the secular part of the perturbation potential for planet i is given, to lowest order in planet masses, m_i, and to lowest order in planetary orbital eccentricities and inclinations, by the following expression

$$\begin{aligned} V_{i,\rm secular} &= -\sum_{j\neq i} \frac{\mathcal{G}m_j}{a_i}\left[\frac{1}{8}\alpha_{ij}\bar{\alpha}_{ij}b^{(1)}_{3/2}(\alpha_{ij})e_i^2 - \frac{1}{4}\alpha_{ij}\bar{\alpha}_{ij}b^{(2)}_{3/2}(\alpha_{ij})e_ie_j\cos(\varpi_i-\varpi_j)\right. \\ &\left. -\frac{1}{8}\alpha_{ij}\bar{\alpha}_{ij}b^{(1)}_{3/2}(\alpha_{ij})s_i^2 + \frac{1}{4}\alpha_{ij}\bar{\alpha}_{ij}b^{(1)}_{3/2}(\alpha_{ij})s_is_j\cos(\Omega_i-\Omega_j)\right], \end{aligned} \tag{27}$$

where $s_j = \sin i_j$, $\varpi_j = \omega_j + \Omega_j$ is the longitude of pericenter,

$$\begin{aligned} \alpha_{ij} &= \min\{a_i/a_j, a_j/a_i\}, \\ \bar{\alpha}_{ij} &= \min\{1, a_i/a_j\}, \end{aligned} \tag{28}$$

and the $b_s^{(k)}$ are Laplace coefficients,

$$b_s^{(k)}(\alpha) \equiv \frac{1}{\pi}\int_0^{2\pi} \frac{\cos k\phi}{(1-2\alpha\cos\phi+\alpha^2)^s}d\phi. \tag{29}$$

Because the secular perturbation potential, Eq. (27), is independent of the mean longitudes ℓ_j, it follows that the canonical momenta L_j are constant. Therefore, the

semimajor axes of the planets are unperturbed and can be treated as fixed parameters (similarly to the stellar and planetary masses). In the secular approximation, only the eccentricities, inclinations, apsides and nodal longitudes are perturbed.

The perturbation analysis is greatly simplified with the use of Poincaré variables representing the *eccentricity vector* and the *inclination vector*,

$$\begin{aligned} h = e\sin\varpi, \qquad & k = e\cos\varpi, \\ p = s\sin\Omega, \qquad & q = s\cos\Omega. \end{aligned} \tag{30}$$

With some straightforward algebra, it is easy to derive that (h, k) are related to the set of canonically conjugate variables,

$$(x, y) = \sqrt{2\Gamma}(\sin\gamma, \cos\gamma) \simeq (Gm_*a)^{1/4}e(-\sin\varpi, \cos\varpi), \tag{31}$$

where x is the coordinate and y is the momentum. Then Hamilton's perturbation equations take the form of linear differential equations with constant coefficients. These can be written succinctly in matrix notation:

$$\frac{d}{dt}\begin{pmatrix} h_1 \\ \vdots \\ h_N \end{pmatrix} = \mathbf{A}\cdot\begin{pmatrix} k_1 \\ \vdots \\ k_N \end{pmatrix}, \qquad \frac{d}{dt}\begin{pmatrix} k_1 \\ \vdots \\ k_N \end{pmatrix} = -\mathbf{A}\cdot\begin{pmatrix} h_1 \\ \vdots \\ h_N \end{pmatrix}, \tag{32}$$

and

$$\frac{d}{dt}\begin{pmatrix} p_1 \\ \vdots \\ p_N \end{pmatrix} = \mathbf{B}\cdot\begin{pmatrix} q_1 \\ \vdots \\ q_N \end{pmatrix}, \qquad \frac{d}{dt}\begin{pmatrix} q_1 \\ \vdots \\ q_N \end{pmatrix} = -\mathbf{B}\cdot\begin{pmatrix} p_1 \\ \vdots \\ p_N \end{pmatrix}. \tag{33}$$

The matrix elements are given by

$$A_{jj} = \frac{1}{4}\sum_{l\neq j}\frac{m_l}{m_*}n_j\alpha_{jl}\bar{\alpha}_{jl}b^{(1)}_{3/2}(\alpha_{jl}), \qquad A_{jl} = -\frac{1}{4}\frac{m_l}{m_*}n_j\alpha_{jl}\bar{\alpha}_{jl}b^{(2)}_{3/2}(\alpha_{jl}), \tag{34}$$

$$B_{jj} = \frac{1}{4}\sum_{l\neq j}\frac{m_l}{m_*}n_j\alpha_{jl}\bar{\alpha}_{jl}b^{(1)}_{3/2}(\alpha_{jl}), \qquad B_{jl} = -\frac{1}{4}\frac{m_l}{m_*}n_j\alpha_{jl}\bar{\alpha}_{jl}b^{(1)}_{3/2}(\alpha_{jl}), \tag{35}$$

where $l \neq j$, and n_j is the unperturbed mean motion of planet j. We note that, to this lowest-order approximation, the equations for h, k are de-coupled from those for p, q.

This is an eigenvalue problem, and the solution takes the simple form of a linear superposition of simple harmonic eigenmodes. Let us denote the eigenfrequencies and eigenmodes of the coefficient matrix $\mathbf{A}$ by g_i and $\mathbf{E}^{(j)}$, respectively, and those for the coefficient matrix $\mathbf{B}$ by f_i and $\mathbf{S}^{(j)}$, respectively. Then the time variation of the eccentricity and inclination vectors are as follows:

$$h_j(t) = \sum_{i=1}^{N} E^{(i)}_j \sin(g_it + \beta_i), \qquad k_j(t) = \sum_{i=1}^{N} E^{(i)}_j \cos(g_it + \beta_i), \tag{36}$$

$$p_j(t) = \sum_{i=1}^{N} S^{(i)}_j \sin(f_it + \gamma_i), \qquad q_j(t) = \sum_{i=1}^{N} S^{(i)}_j \cos(f_it + \gamma_i). \tag{37}$$

The solution involves arbitrary constants – the magnitudes of the eigenvectors, $|\mathbf{E}^{(i)}|, |\mathbf{S}^{(i)}|$, and the phases β_i and γ_i – which are determined by the initial conditions $h_i(0), k_i(0)$ and $p_i(0), q_i(0)$.

To summarize, the secular variation of the eccentricity vector (respectively, inclination vector), of each planet is a superposition of eigenmodes. Analogous secular behavior obtains for the inclination vectors, but with one difference: one of the eigenmodes has vanishing frequency, owing to the conservation of total angular momentum. Therefore, the eccentricities and inclinations of the planets vary with time, and the pericenter and nodal longitudes precess, quasi-periodically, on timescales of order $\sim g_l^{-1}$.

In the solar system, the linear secular theory for the eight major planets (Mercury, Venus, ..., Neptune) has frequencies g_i in the magnitude range of about 0.7–28 arcsec per year; the magnitude range of the inclination frequencies, f_i, is similar, save for $f_5 = 0$. Thus the timescales of secular variations of the planetary eccentricities and inclinations in the solar system range from about 46,000 years to about 1.8 million years.

Eccentricity secular resonance for a minor planet

We now turn to examining the orbit of a test particle that is subject to the perturbations of planets whose orbits undergo the above secular perturbations. As above, we consider these perturbations to lowest order in orbital eccentricities, inclinations and in planet masses. In this approximation, the eccentricities and inclination perturbations are decoupled. Let us consider the eccentricity perturbations.

The eccentricity perturbations of the test particle's orbit are described by the sum of the perturbations arising from each planet:

$$V_{\rm tp,sec} = -\sum_{j=1}^{N} \frac{\mathcal{G}m_j}{a} \left\{ \frac{1}{8}\alpha_j\bar{\alpha}_j b^{(1)}_{3/2}(\alpha_j)e^2 - \frac{1}{4}\alpha_j\bar{\alpha}_j b^{(2)}_{3/2}(\alpha_j)ee_j\cos(\varpi_{\rm j} - \varpi) \right\}, \tag{38}$$

where $\alpha_j = \min\{a/a_{\rm j}, a_{\rm j}/a\}, \bar{\alpha}_j = \min\{1, a/a_j\}$, and e is the eccentricity of the test particle's orbit. We can make use of the Poincaré variables, (h, k), and substitute in Eq. (38) the secular solution for the planets, Eq. (36), so that the perturbation potential is expressed as follows:

$$\begin{aligned} V_{\rm tp,sec} \;=\; & -\textstyle\sum_{j=1}^{N} \frac{\mathcal{G}m_j}{8a}\alpha_j\bar{\alpha}_j b^{(1)}_{3/2}(\alpha_j)(h^2+k^2) \\ & + \textstyle\sum_{l=1}^{N}\sum_{j=1}^{N} \frac{\mathcal{G}m_j}{4a}\alpha_j\bar{\alpha}_j b^{(2)}_{3/2}(\alpha_j)E^{(l)}_j[k\cos(g_l t+\beta_l) - h\sin(g_l t+\beta_l)]. \end{aligned} \tag{39}$$

Following the same procedure as for the secular theory for the planets, we relate the canonical set $\sqrt{2\Gamma}(\sin\gamma, \cos\gamma)$ to (h, k), and use Hamilton's equations to obtain the following equations of motion for the test particle's eccentricity vector:

$$\dot{h} = g_0 k - \sum_{l=1}^{N} F_l\cos(g_l t+\beta_l), \qquad \dot{k} = -g_0 h + \sum_{l=1}^{N} F_l\sin(g_l t+\beta_l), \tag{40}$$

where

$$g_0 = \frac{n}{4}\sum_{j=1}^{N}\frac{m_j}{m_*}\alpha_j\bar{\alpha}_j b_{3/2}^{(1)}(\alpha_j), \qquad F_l = \frac{n}{8}\sum_{j=1}^{N}\frac{m_j}{m_*}\alpha_j\bar{\alpha}_j b_{3/2}^{(2)}(\alpha_j)E_j^{(l)}. \tag{41}$$

These equations are qualitatively similar to those for a harmonic oscillator of natural frequency g_0 driven at N discrete external forcing frequencies, g_l. The general solution is a sum of the free and forced oscillations, with the latter given by

$$\Big\{h(t), k(t)\Big\}_{\rm forced} = \sum_{l=1}^{N}\frac{F_l}{g_0 - g_l}\Big\{\sin(g_l t + \beta_l), \cos(g_l t + \beta_l)\Big\}. \tag{42}$$

For given fixed parameters of the planetary system, the amplitude of the forced oscillations depends only upon the semimajor axis, a, of the test particle. From Eq. (42), we can anticipate that for some values of a the 'natural frequency' g_0 is nearly equal to one of the planetary secular mode frequencies, g_l. At exact resonance, i.e. $g_0 = g_1$, we have the particular solution of the resonantly forced oscillations whose amplitude grows without bound:

$$\Big\{h(t), k(t)\Big\}_{\rm resonance} \simeq tF_l\Big\{-\cos(g_l t + \beta_l), \sin(g_l t + \beta_l)\Big\}. \tag{43}$$

The timescale for the growth of the amplitude, $\sim F_l^{-1}$, is inversely related to the masses and eccentricities of the planets.

Examples of minor planets at secular resonances

A prominent example of a linear secular resonance occurs in the inner solar system at approximately 2 AU heliocentric distance. At this location, a minor planet in a nearly circular orbit has a 'natural' apsidal frequency $g_0 \approx 28''/\text{yr}$, very nearly the same as the largest frequency, $g_6 \simeq 28.25''/\text{yr}$, of the major planets' eccentricity secular modes. This is known as the ν_6 secular resonance; it has an associated timescale for eccentricity growth of $\sim 10^5$ yr. In the Kuiper belt, a similarly prominent secular resonance is the so-called ν_8 secular resonance which is defined by $g_0 \approx g_8$. The latter is the lowest secular frequency of the planetary eccentricities. The timescale of eccentricity growth in the ν_8 resonance is $\sim 10^7$ yr. The forced eccentricity of test particles near the ν_6 resonance in the asteroid belt, and near the ν_8 resonance in the Kuiper belt are plotted in Figure 4. Observationally, the location of the ν_6 resonance coincides with the inner boundary of the main asteroid belt, and the location of the ν_8 resonance coincides with a gap in the distribution of Kuiper belt objects. A number of numerical studies have shown that the ν_6 resonance provides a dynamical transport route for meteorite delivery to Earth, for asteroid fragments that are injected into the ν_6 resonance by means of random collisions or other perturbations elsewhere in the main asteroid belt. A similar phenomenon may be at work to inject Kuiper belt objects into high eccentricity Neptune-crossing orbits via the ν_8 resonance, and these may contribute to the supply of short period comets from the Kuiper belt to the inner solar system.

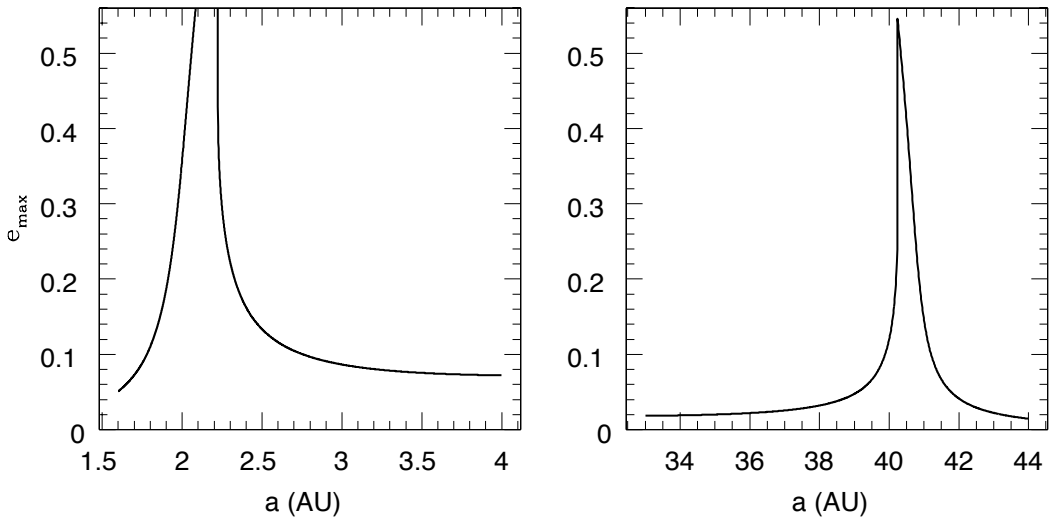

Figure 4: Forced eccentricity of test particle orbits near the ν_6 resonance in the asteroid belt (left), and near the ν_8 resonance in the Kuiper Belt (right).

Secular resonances also occur embedded within or in close proximity to mean motion resonances in the asteroid belt as well as in the Kuiper Belt, with interesting implications for the long term stability of minor planet populations at mean motion resonances.

The instability of circular orbits caused by a secular resonance can be used to constrain the locations and masses of unseen planets or planetesimal belts in extra-solar systems. One such example is the two-planet system known as OGLE-2006-BLG-109L, recently discovered by means of microlensing observations; the secular perturbation theory analysis of the system has been used to constrain the orbit and mass of a habitable zone terrestrial planet in this system.

2.3 Sweeping secular resonance

We noted in the previous section that the stellar mass and the planetary masses and orbital semimajor axes are 'fixed' parameters of the secular perturbation analysis. However, in the early history of a planetary system, some of these parameters are subject to changes. Such time variability of these parameters causes the secular resonance locations to sweep across large regions of minor planets' parameter space, causing large perturbations on entire populations of minor planets.

Sweeping, or scanning, secular resonances are of interest in a number of contexts in the solar system and may well find application in exo-planetary systems in the future. Sweeping secular resonances due to the changing quadrupole moment of the Sun during solar spin-down have been explored as a possible mechanism for explaining the eccentricity and inclination of Mercury. Secular resonance sweeping due to the effects

of the dissipating solar nebula just after planet formation has also been investigated as a possible mechanism for exciting the orbital eccentricities of Mars and of the asteroid belt. The dissipating massive gaseous solar nebula would have altered the secular frequencies of the solar system planets in a time-dependent way, causing locations of secular resonances to possibly sweep across the inner solar system, thereby exciting asteroids as well as the small planets, Mercury and Mars, into the eccentric and inclined orbits that are observed today. However, the quantitative predictions of such a mechanism appear to not account very well for observations, and this remains an outstanding problem.

Here we consider the secular resonance sweeping driven by the orbital migration of planets, and its effects on a belt of planetesimals. We assume that the planetesimals have negligible mass compared to the planets, so they can be treated as infinitesimal mass test particles. Consider a ν_p resonance defined by $g_0 \approx g_p$, where g_p is one of the secular mode frequencies of the planets. Then we can neglect all but the $l = p$ term in the perturbation potential, Eq. (39). A natural new set of *resonant variables* is then defined by

$$x = e\cos(\varpi - g_p t - \beta_p), \quad y = e\sin(\varpi - g_p t - \beta_p). \tag{44}$$

Furthermore, we make the simplification that the dominant and only effect of the orbital migration of the planets is that the difference frequency, $g_0 - g_p$ is a slowly varying parameter, with

$$\dot{g}_0 - \dot{g}_p = 2\lambda = \text{constant}. \tag{45}$$

It is then straightforward to find that the equations of motion for the resonant variables are given by

$$\dot{x} = 2\lambda t y; \qquad \dot{y} = -2\lambda t x + F_p, \tag{46}$$

where we have defined, without loss of generality, $t = 0$ as the time of exact resonance crossing when $g_0 = g_p$. These equations of motion form a system of nonhomogenous linear differential equations. The general solution is given by a linear combination of a homogeneous solution and a particular solution:

$$\begin{aligned} x(t) &= x_i \cos\left[\lambda\left(t^2 - t_i^2\right)\right] + y_i \sin\left[\lambda\left(t^2 - t_i^2\right)\right] \\ &\quad + \frac{\varepsilon}{\sqrt{|\lambda|}}\left[(S - S_i)\cos\lambda t^2 - (C - C_i)\sin\lambda t^2\right], \end{aligned} \tag{47}$$

$$\begin{aligned} y(t) &= -x_i \sin\left[\lambda\left(t^2 - t_i^2\right)\right] + y_i \cos\left[\lambda\left(t^2 - t_i^2\right)\right] \\ &\quad - \frac{\varepsilon}{\sqrt{|\lambda|}}\left[(C - C_i)\cos\lambda t^2 + (S - S_i)\sin\lambda t^2\right]. \end{aligned} \tag{48}$$

Here $x_i = x(t_i), y_i = y(t_i)$ are the initial conditions at the initial time t_i (long before resonance crossing, $t_i \to -\infty$), and $S = S(t), C = C(t)$ are the Fresnel integrals,

$$S(t) = \int_0^t \sin t'^2 dt', \qquad C(t) = \int_0^t \cos t'^2 dt'. \tag{49}$$

We can find the change in x and y owed to the resonance sweeping by evaluating $(x(t), y(t))$ long after resonance encounter ($t \to +\infty$):

$$\begin{aligned} x_f &= x_i + F_p \sqrt{\frac{\pi}{2|\lambda|}} \left[\cos \lambda t_i^2 - \sin \lambda t_i^2 \right], \\ y_f &= y_i - F_p \sqrt{\frac{\pi}{2|\lambda|}} \left[\cos \lambda t_i^2 + \sin \lambda t_i^2 \right], \end{aligned} \tag{50}$$

where we have made use of the limiting value of the Fresnel integrals, $S(\infty) = C(\infty) = \sqrt{\pi/8}$. This yields the change in the eccentricity due to the resonance sweeping:

$$e_f^2 = e_i^2 + \frac{\pi F_p^2}{|\lambda|} + 2F_p \sqrt{\frac{\pi}{|\lambda|}} e_i \cos \varpi_i. \tag{51}$$

For non-zero initial eccentricity, the phase dependence in Eq. (51) means that secular resonance sweeping can both increase and reduce orbital eccentricities. Considering all possible values of $\cos \varpi_i$ in the range $\{-1, +1\}$, a minor planet with initial eccentricity e_i that is swept by the ν_p secular resonance will have a final eccentricity in the range e_{min} to e_{max}, where

$$e_{min,max} \simeq |e_i \pm \delta_e|, \tag{52}$$

and

$$\delta_e \equiv \left| F_p \sqrt{\frac{\pi}{|\lambda|}} \right|. \tag{53}$$

Note that the magnitude of eccentricity change is inversely related to the speed of planet migration.

For illustration, Figure 5 plots the analytically predicted time evolution of the eccentricity of an ensemble of asteroids subjected to the sweeping of the ν_6 secular resonance when Saturn's orbit migrates outward by about 1 AU in 1 million years. Initially, the asteroids all started with a common value of the semimajor axis and eccentricity, but different values of the longitude of pericenter (randomly distributed in the range 0–2π).

Equations (51)–(53) have the following implications: (i) Initially circular orbits become eccentric, with a final eccentricity δ_e. (ii) An ensemble of minor planets near the same semimajor axis and with the same initial non-zero eccentricity but uniform random orientations of pericenter is transformed into an ensemble that has eccentricities in the range e_{min} to e_{max}; this range is not uniformly distributed because of the $\cos \varpi_i$ dependence in Eq. (51), rather the distribution peaks at the extreme values.

Analogous results obtain for the sweeping of an inclination secular resonance.

In the solar system, there is some evidence for a double-peaked eccentricity distribution in the asteroid belt and a double peaked inclination distribution in the Kuiper belt. Relating these observations to the early orbital migration of the giant planets is an active area of research at present.

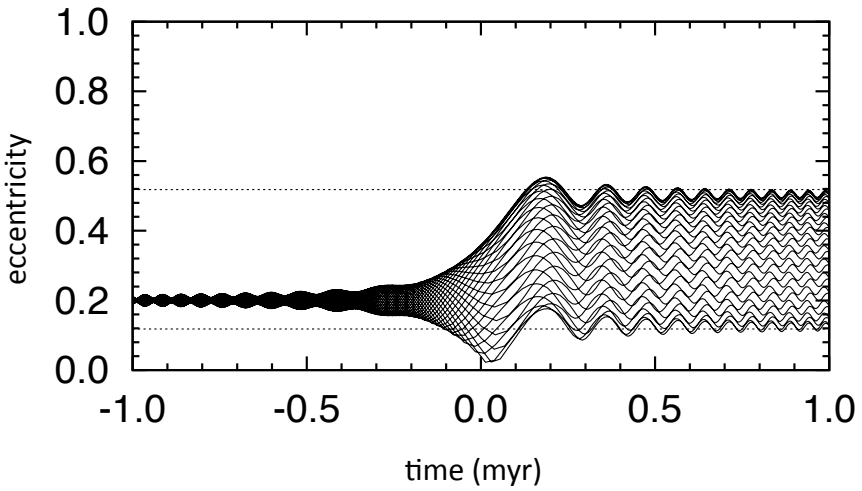

Figure 5: The evolution of the eccentricity of an ensemble of asteroids subjected to ν_6 secular resonance sweeping, as determined by equations 47–50. The ensemble starts with the same values of semimajor axis and eccentricity, but random values of the longitude of pericenter.

3 Mean motion resonances

3.1 Single resonance theory

The simplest case of a mean motion resonance occurs in the planar circular restricted three-body problem in which a single planet orbits a star in a circular orbit and a test particle orbits the star with an orbital period close to a ratio of small integers, $p : p + q$, with $p \neq 0$ and $q \geq 0$. Recall that the Hamiltonian for the test particle is given by the sum of its unperturbed Keplerian Hamiltonian and an interaction Hamiltonian describing the perturbations from the planet; we can express this in terms of the modified Delaunay variables $\Lambda, \Gamma, \lambda, \gamma$:

$$\begin{aligned} \mathcal{H}(\lambda, \gamma, \Lambda, \Gamma, t) &= -\frac{(\mathcal{G}m_*)^2}{2\Lambda^2} - \mathcal{G}m_{\rm p}\left[\frac{1}{|\mathbf{r} - \mathbf{r}_{\rm p}|} - \frac{\mathbf{r}\cdot\mathbf{r}_{\rm p}}{r_{\rm p}^3}\right] \\ &= -\frac{(\mathcal{G}m_*)^2}{2\Lambda^2} + \mathcal{H}_{\rm p}(\lambda, \gamma, \Lambda, \Gamma, a_{\rm p}, t) \end{aligned} \tag{54}$$

where $\mathbf{r}, \mathbf{r}_{\rm p}$ are, respectively, the position vectors of the test particle and planet relative to the star and H_p represents the planetary perturbation.

Let us examine the dynamics near a first order mean motion resonance, $q = 1$. It is useful to make a canonical transformation to slow and fast variables,

$$\begin{aligned} \phi &= (p+1)\lambda_{\rm p} - p\lambda + \gamma, \qquad \Phi = \Gamma, \\ \psi &= \lambda - \lambda_{\rm p}, \qquad\qquad\qquad \Psi = \Lambda + p\Gamma, \end{aligned} \tag{55}$$

where $\lambda_p = n_{\rm p}(t - t_0)$ is the mean longitude of the planet, and $n_{\rm p}$ is its mean motion. Then the new Hamiltonian is

$$\begin{aligned} \widetilde{H} &= n_{\rm p}[(p+1)\Phi - \Psi] - \frac{\mu^2}{2(\Psi - p\Phi)^2} \\ &\quad + \widetilde{\mathcal{H}}_{\rm p}(\phi, \psi, \Phi, \Psi; a_{\rm p}) \end{aligned} \tag{56}$$

where $a_{\rm p}$ is the semi-major axis of the planet's orbit. Close to resonance, ψ is a fast variable (relative to ϕ), we will drop the ψ-dependent terms. Consequently, the resonant Hamiltonian is independent of ψ, thus Ψ is a constant of the motion. The following auxiliary constants are useful for notational simplication:

$$n_* = \frac{(\mathcal{G}m_*)^2}{\Psi^3}, \qquad a_* = \frac{\Psi^2}{\mathcal{G}m_*}; \tag{57}$$

n_* and a_* are constants of the motion which equal the osculating mean motion and semi-major axis of the test particle when its eccentricity is zero.

If the test particle orbit is nearly circular, then $\Phi \simeq \frac{1}{2}\sqrt{\mathcal{G}m_* a}e^2$ is small, and we can approximate Eq. (56) with a few terms in an expansion in powers of $\sqrt{\Phi}$,

$$\widetilde{\mathcal{H}}_{\rm res} = [(p+1)n_{\rm p} - pn_*]\Phi + \beta\Phi^2 + \varepsilon\sqrt{2\Phi}\cos\phi, \tag{58}$$

where we have dropped an inessential constant, and

$$\beta = -\frac{3p^2 n_*}{2\Psi}, \qquad \varepsilon = -\frac{\mathcal{G}m_{\rm p}}{a_{\rm p}}\frac{f_p}{\sqrt{\Psi}}. \tag{59}$$

Note that $\Psi \simeq \sqrt{\mathcal{G}m_* a}(1 + \frac{1}{2}pe^2)$, and since the eccentricity is small, we have $\Psi > 0$ and $\beta < 0$ in all cases of interest. The coefficient f_p is given by

$$f_p = \left\{ \begin{array}{lll} -(p + 1 + \frac{1}{2}D)b_{1/2}^{(p+1)}(\alpha), & \alpha = (1+1/p)^{-2/3} & \text{for } p > 0, \\ -\alpha(p + \frac{1}{2} - \frac{1}{2}D)b_{1/2}^{(|p+1|)}(\alpha) - \frac{\delta_{p,-2}}{2\alpha}, & \alpha = (1+1/p)^{2/3} & \text{for } p < 0. \end{array} \right\} \tag{60}$$

Here $\delta_{i,j}$ is the Kronecker delta function, $D \equiv d/d\log\alpha$, and $b_{1/2}^{(p)}$ is a Laplace coefficient.

For a universal description of any first order resonance, it is useful to define a dimensionless canonical momentum, R, and a modified canonical coordinate θ,

$$R = \left|\frac{2\beta}{\varepsilon}\right|^{2/3}\Phi, \qquad \theta = \left\{ \begin{array}{ll} -\phi & \text{if } \varepsilon > 0, \\ \pi - \phi & \text{if } \varepsilon < 0. \end{array} \right. \tag{61}$$

For small eccentricity, we can write $2R \simeq (e/s_e)^2$, where the eccentricity scale is

$$s_e \equiv \frac{1}{(\mu a_*)^{1/4}}\left|\frac{\varepsilon}{2\beta}\right|^{1/3} = \left|\frac{m_{\rm p} a_* f_p}{3p^2 m_* a_{\rm p}}\right|^{1/3}. \tag{62}$$

The dimensionless Hamiltonian in the canonical variables (θ, R) is then given by

$$K = -3\Delta R + R^2 - 2\sqrt{2R}\cos\theta, \tag{63}$$

where the dimensionless parameter, Δ, is a measure of the closeness to exact resonance,

$$\Delta = \frac{(p+1)n_{\rm p} - pn_*}{s_\nu}, \tag{64}$$

and s_ν is a frequency scale,

$$s_\nu \equiv \left|\frac{27\beta\varepsilon^2}{4}\right|^{1/3} = \left|\frac{9pm_{\rm p}a_* f_p}{\sqrt{8}a_{\rm p}m_*}\right|^{2/3} n_*. \tag{65}$$

For eccentricity $e \to 0$, $n_* = n$ is the unperturbed mean motion, and the "exact resonance" condition $pn_* = (p+1)n_{\rm p}$ corresponds to $\Delta = 0$. The small amplitude libration frequency of the resonant angle is of order $\sim s_\nu$.

The above analysis provides several useful results in understanding resonant dynamics.

The first integral, $\Psi = \sqrt{\mathcal{G}m_* a}(1 - p(1 - \sqrt{1-e^2}))$, defines a relationship between the resonant perturbations of the mean motion and eccentricity:

$$\frac{\delta n}{n} = -\frac{3\delta a}{2a} \approx \frac{3p}{2}\delta e^2, \tag{66}$$

which shows that the resonant perturbations in a are much smaller than those in e.

The range of the resonant perturbation is $|(p+1)n_{\rm p} - pn_*| \sim |p| s_\nu$. This means that the "width" of the resonance is proportional to $m_{\rm p}^{2/3}$.

The topology of the phase space determined by the dimensionless resonant Hamiltonian depends only upon the value of Δ.

The phase space trajectories follow level curves of the dimensionless resonant Hamiltonian K, Eq. (63). Figure 6 shows plots of the level curves for various values of Δ to illustrate the phase space topology. In these plots, we use the Poincaré variables $(x, y) = \sqrt{2R}(\cos\theta, \sin\theta)$, which are also canonical (y is the coordinate and x is the conjugate momentum). The origin in these plots corresponds to zero eccentricity, and the distance from the origin is e/s_e.

The phase space structure is very simple when $|\Delta| \gg 1$: the trajectories are nearly circles centered close to the origin. For $\Delta < 1$, there is only one fixed point and no homoclinic trajectory, but for $\Delta > 1$ there are three fixed points and a homoclinic trajectory (a separatrix) exists. All the fixed points are on the x-axis; they are given by the solutions of $\partial K/\partial x = 0$ which are the real roots of the cubic equation

$$x^3 - 3\Delta x - 2 = 0. \tag{67}$$

Figure 7 plots the locations of the real roots as a function of Δ.

The separatrix, when it exists, divides the phase space into three zones: an external and an internal zone and a 'resonance' zone. Most orbits in the resonance zone are librating orbits, i.e. the resonant angle, θ (equivalently, ϕ), executes finite amplitude oscillations, whereas most orbits in the external and internal zones are circulating orbits (i.e. the resonant angle increases or decreases without bound).

For *initially circular orbits*, there are several interesting properties:

- For $|\Delta| \gg 1$, the resonantly forced oscillations in (x, y) of particles on initially circular orbits are nearly sinusoidal, with frequency 3Δ and amplitude $\sim \frac{2}{3}|\Delta|^{-1}$.
- In the vicinity of $\Delta \approx 0$, the oscillations are markedly non-sinusoidal, and have a maximum amplitude of $2^{\frac{5}{3}}$ at $\Delta = 2^{\frac{1}{3}}$. Thus, the maximum eccentricity excitation of initially circular orbits is

$$e_{\max} \simeq 2^{\frac{5}{3}} s_e \qquad \text{for } e_i = 0. \tag{68}$$

  The behavior of initially circular orbits is discontinuous near $\Delta = 2^{\frac{1}{3}}$: the oscillation amplitude is $2^{\frac{5}{3}}$ for Δ just below $2^{\frac{1}{3}}$, but the amplitude is just half that value, $2^{\frac{2}{3}}$, for Δ just above $2^{\frac{1}{3}}$. (We note in passing that $\Delta = 2^{\frac{1}{3}}$ represents a period-doubling transition point.) Figure 8 illustrates this behavior.
- The half-maximum amplitude occurs at a value of $\Delta \simeq -0.42$. Thus, we can define the resonance full-width-at-half-maximum amplitude in terms of the mean motion of the test particle

$$\Delta n \approx \frac{2}{|p|} s_\nu = \left| \frac{9 m_{\rm p} a_* f_p}{\sqrt{8|p|} a_{\rm p} m_*} \right|^{2/3} n_*. \tag{69}$$

3.2 Resonance Capture

The behavior of initially circular orbits to adiabatic changes of Δ (due to external forces) is of particular interest in the evolution of orbits near mean motion resonances in the presence of small dissipative forces. Of course, in the presence of dissipation, the actual trajectories are not closed in the (x, y) phase plane, but the level curves of the single resonance Hamiltonian (Figure 6) serve as 'guiding' trajectories for such dissipative evolution. We can gain considerable insight into the evolution near resonance by using the property that the action is an adiabatic invariant of the motion in a Hamiltonian system. For the single resonance Hamiltonian, the action is simply the area enclosed by a phase space trajectory in the (x, y) plane. Therefore, for guiding trajectories which remain away from the separatrix, adiabatic changes in Δ preserve the area enclosed by the guiding trajectory in the (x, y) phase plane, even as the guiding center moves. There are two possible guiding centers corresponding to the two centers of libration of θ (which occur on the x-axis, i.e. at $\theta = 0$ or π, Figure 6). In Figure 7, the locations of the libration centers are the fixed points x_1 and x_2, plotted as a function of Δ.

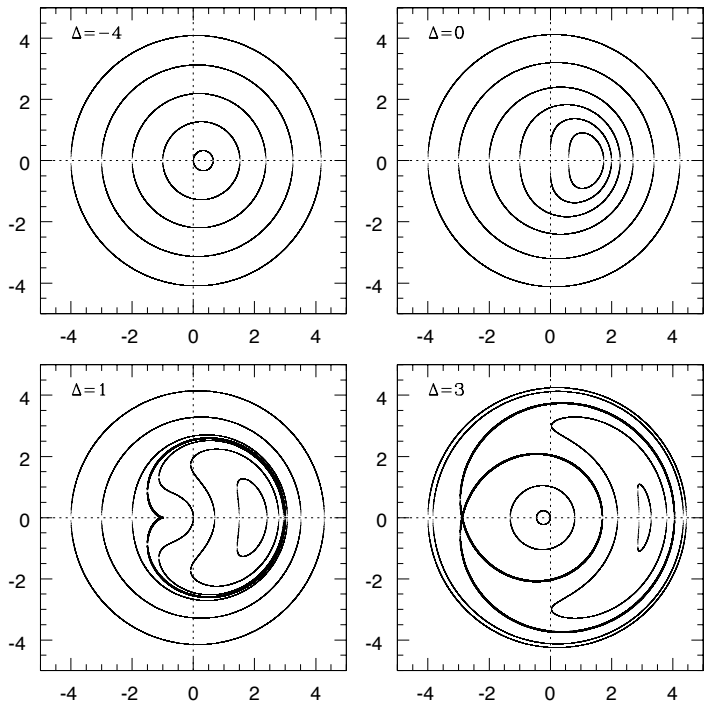

Figure 6: Level curves of the dimensionless resonant Hamiltonian, Eq. (63), for various values of the resonance distance Δ, Eq. (64). The coordinates are $(x, y) = \sqrt{2R}(\cos\theta, \sin\theta)$.

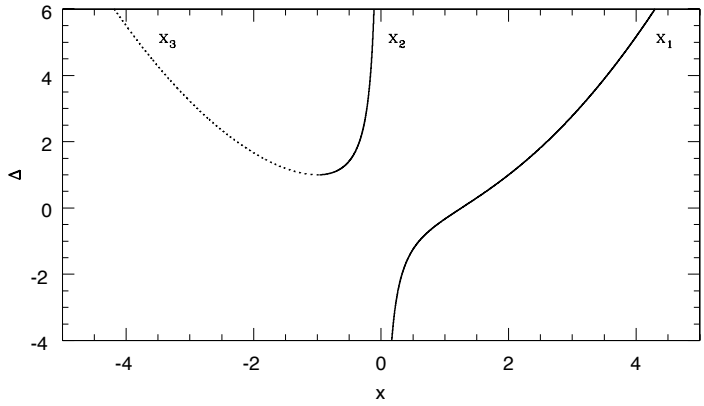

Figure 7: Fixed points of the dimensionless Hamiltonian for a first order resonance, Eq. (63), as a function of the resonance distance Δ. The fixed points have $\theta = 0$ or π and the variable plotted is $x = \sqrt{2R}\cos\theta$. For $\Delta > 1$, the unstable fixed point that lies on the separatrix is shown as a dotted line.

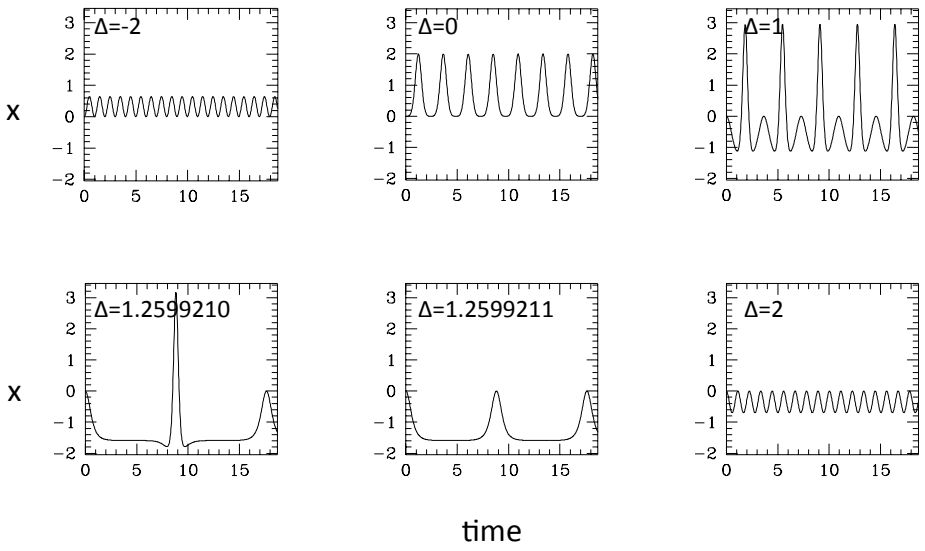

Figure 8: The time evolution of the variable $x = \sqrt{2R}\cos\theta$ for an initially circular orbit, for several values of Δ.

Convergent evolution

Consider a particle initially in a circular orbit whose orbit frequency approaches that of the planet's orbit frequency. This particle will approach the resonance from the left, i.e. Δ increasing from initially large negative values, and its initial guiding trajectory has zero enclosed area. The initial "free eccentricity" is vanishingly small, and the particle's eccentricity is determined by the resonant forcing alone. Such an orbit adiabatically follows the positive branch, x_1, in Figure 7, so that as Δ evolves to large positive values, the particle's eccentricity is adiabatically forced to large values as the guiding center moves away from the origin. We have

$$x_1 \simeq \sqrt{3\Delta} \quad \text{for} \quad \Delta \gg 1. \tag{70}$$

Recall that x is the dimensionless eccentricity. Thus, the rate of increase of the resonantly forced [dimensionless] eccentricity along the positive branch is given by

$$\frac{dx_1^2}{dt} \simeq 3\frac{d\Delta}{dt}\bigg|_{\rm ext}, \tag{71}$$

where the subscript 'ext' refers to the effect of external dissipative forces.

The guiding trajectory will be forced to cross the separatrix if the initial area enclosed by it exceeds $A_1 = 6\pi$, the area enclosed by the separatrix when it first appears at $\Delta = 1$. This defines a critical eccentricity,

$$e_{\rm crit} = \sqrt{6}s_e. \tag{72}$$

For initial eccentricity $e_i < e_{\rm crit}$, capture into resonance is assured as Δ increases adiabatically from initially large negative values to positive values, whereas for $e_i > e_{\rm crit}$, the test particle will encounter a separatrix.

Negotiating the separatrix is difficult business, for the adiabatic invariance of the action breaks down close to the separatrix where the period of the guiding trajectory becomes arbitrarily long. However, the crossing time is finite in practice, and separatrix crossing leads to a quasi-discontinuous "jump" in the action; subsequently, the new action is again an adiabatic invariant. There are two possible outcomes: the final guiding trajectory can be either in the resonance zone or in the internal zone. It is possible to compute a probability of transition for the two possible outcomes by assuming a random phase of encounter of the guiding trajectory with the separatrix.

Divergent evolution

Finally, consider a particle initially in a circular orbit whose orbit frequency diverges slowly from that of the planet's orbit frequency. This particle will approach the resonance from the right, with Δ decreasing from initially large positive values. In this case, the guiding trajectory adiabatically follows the negative branch, x_2, in Figure 7. However, the center of librations on the negative branch merges with the unstable fixed point on the separatrix at $\Delta = 1$, and the guiding trajectory is forced to negotiate the separatrix. There occurs a discontinuous change in the guiding trajectory which becomes briefly nearly coincident with the separatrix. Thereafter, as Δ continues to decrease, the separatrix disappears, and the guiding trajectory becomes increasingly circular about the origin, with an area equal to 6π, which is the area enclosed by the separatrix at $\Delta = 1$. Thus, in this case, passage through resonance leaves the particle with an excited "free eccentricity" equal to $e_{\rm crit}$ (Eq. (72)).

3.3 Overlapping mean motion resonances and Chaos

In the previous sections, we analyzed the dynamics of a single first order $p : p+1$ mean motion resonance, treated in isolation. In reality, there exists an infinite sequence of resonances in the restricted three-body problem,

$$2:1,\ 3:2,\ 4:3,\ 5:4,\ \ldots \qquad \text{interior resonances, } p > 0 \tag{73}$$

$$1:2,\ 2:3,\ 3:4,\ 4:5,\ \ldots \qquad \text{exterior resonances, } p < 0. \tag{74}$$

The separation between two neighboring first order resonances, $p : p+1$ and $p+1 : p+2$, is given by

$$\delta n = \Big(\frac{p+1}{p+2} - \frac{p}{p+1}\Big) n_{\rm p} \approx p^{-2} n_{\rm p}. \tag{75}$$

The separation between resonances decreases as $|p|$ increases. When the separation between neighboring resonances becomes similar to their widths, the single resonance theory breaks down. The nature of this breakdown is revealed in numerical solutions: large

scale chaotic behavior of orbits. Overlapping resonances are a universal route to stochastic (chaotic) behavior in dynamical systems.

For nearly circular orbits, we have derived the width of each resonance, Eq. (69). For $p \gg 1$, the resonant coefficient, f_p defined in Eq. (60) has the following simple approximation:

$$f_p \simeq -\frac{p}{\pi}[2K_0(2/3) + K_1(2/3)] \simeq 0.80\, p, \tag{76}$$

where K_i are modified Bessel functions. With this approximation, the sum of the half-widths of neighboring mean motion resonances from Eq. (69) is

$$\Delta n \approx 3.73\, p^{\frac{1}{3}} \mu^{\frac{2}{3}}\, n_{\rm p}, \tag{77}$$

where $\mu = m_{\rm p}/m_*$. An examination of Eqns. 75 and 77 shows that for a given m_p there exists some value $p_{\rm min}$ such that the widths of first order resonances close to the planet with $|p| > p_{\rm min}$ will exceed their separation. In this region, which is approximately an annular region around the planet's orbit, initially circular orbits will exhibit the universal chaotic instability that arises from overlapping resonances.

More precisely, let us define the overlap ratio:

$$\gamma \equiv \frac{\Delta n}{\delta n}. \tag{78}$$

The "two-thirds" rule states that the chaotic layers at the resonance separatrices merge — and most orbits in the vicinity of the resonances will be chaotic — when the overlap ratio γ is $\gtrsim 2/3$, i.e.

$$|p|^{-1} \lesssim 2.1\mu^{2/7}. \tag{79}$$

For $|p| \gg 1$, we have $|p|^{-1} \simeq \delta a/a_p$, where $a_p + \delta a = ((p+1)/p)^{2/3}$ is the semimajor axis of the exact resonant orbit. Thus, we can define the width of the annular region, $\Delta a_{\rm ro}$, where first order resonances overlap according to the "two-thirds" rule:

$$\Delta a_{\rm ro} \simeq 1.4\mu^{\frac{2}{7}} a_p. \tag{80}$$

The above equation estimates the extent of the chaotic region in the vicinity of a planet's orbit where circular test particle orbits are unstable and exhibit strongly chaotic behavior. Figure 9 provides an illustration of the phenomenon of first order mean motion resonance overlap. We see that for mass ratio $\mu = 1 \times 10^{-5}$, the 8:7 and 7:6 neighboring mean motion resonances are well separated, with only a very thin chaotic zone near their separatrices. However, for a slightly larger mass ratio, $\mu = 2.5 \times 10^{-5}$, separatrices of these resonances broaden and merge into a large chaotic zone.

The chaotic zone defined by the resonance overlap region does not preclude the existence of small regions of quasiperiodic orbits embedded within it. Obvious examples are the stable libration zones at the classical Lagrangian points where the mean motion of test particles is in 1:1 resonance with that of the planet. Small libration zones persist in the vicinity of other mean motion resonances as well, such as indicated in Figure 9.

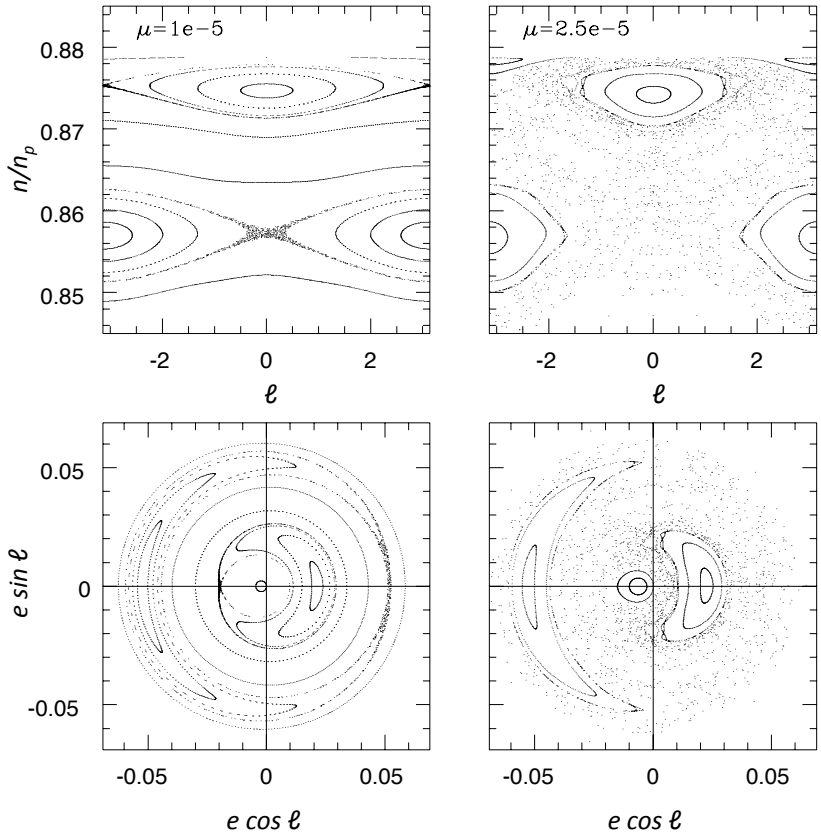

Figure 9: Surfaces-of-section for the circular planar three-body problem illustrating the merging of the 7/6 and the 8/7 mean motion resonance separatrices as the mass ratio $m_{\rm p}/m_*$ increases from 1×10^{-5} (left) to 2.5×10^{-5} (right). The upper and lower panels represent views of the same orbits, plotted in different variables.

Mean motion resonances outside the $\mu^{\frac{2}{7}}$ chaotic zone also have chaotic layers in the vicinity of their separatrices, with layer thickness diminishing with mean distance from the planet but a strong function of the mean eccentricity.

4 Epilogue

Orbital resonances are a source of both stability and chaos, depending sensitively upon parameters and initial conditions. This fundamental conclusion and an understanding of its implications is leading a resurgence in the field of celestial mechanics, with import for planetary science in general. We have provided here an overview of orbital resonance phenomena, with simple models that guide our understanding. The progress in recent

years has already led to new insights on the origin of orbital configurations in the solar system and in extra-solar planetary systems. In the near future, we anticipate much progress in planetary dynamics, particularly in regard to the origin and evolution of the orbital characteristics of planetary systems viewed as an ensemble.

Glossary

Completely integrable system: an n–dimensional Hamiltonian system admitting n first integrals in involution and independent.

Kepler's laws: a set of three laws devised by Johannes Kepler to describe the motion of a celestial body in the gravitational field of a primary body.

Lagrangian points: the equilibrium points of the three–body problem in a synodic (rotating) reference frame. Three equilibrium positions are referred to as *collinear,* since they lie on the direction joining the primaries; two equilibrium positions are called *triangular,* since they form an equilateral triangle with the primaries.

Pericenter: the point on the elliptical orbit of a celestial body which is at the minimum distance from the focus.

Perturbation theory: a constructive theory which allows to provide an approximate solution to the equations of motion of a nearly–integrable system.

Quasi–periodic motion: conditionally periodic motion with incommensurable frequencies.

Resonance: a commensurability condition among the frequencies of a dynamical system.

Secular Resonance: a commensurability condition among the slow frequencies of precession of the apsides or and/or the nodes in a planetary system.

Biographical sketch

Renu Malhotra (born in 1961 in New Delhi, India) earned her M.S. in Physics from the Indian Institute of Technology in Delhi in 1983, and her Ph.D. in Physics from Cornell University in 1988. She did post-doctoral research at Cornell and at Caltech, and worked as a staff scientist at the Lunar and Planetary Institute in Houston. In 2000 she joined the faculty of The University of Arizona in Tucson, where she is currently Professor and Chair of the Theoretical Astrophysics Program. Her research in orbital mechanics has spanned a wide variety of topics, including extra-solar planets and debris disks around stars, the formation and evolution of the Kuiper belt and the asteroid belt, the orbital resonances amongst the moons of the giant planets, and the meteoritic bombardment history of the planets. She has revolutionized our understanding of the early history of the solar system by using the orbital resonance between Pluto and Neptune to infer large-scale orbital migration of the giant planets and to predict the existence of the "Plutinos"

and other small planets in resonance with Neptune. She has been the recipient of honors and awards from the American Astronomical Society (Harold C. Urey Prize, 1997), the International Astronomical Union (asteroid 6698 named 'Malhotra', 1997), the IIT-Delhi (Distinguished Alumna, 2006) and The University of Arizona (Galileo Fellow, 2010).

Bibliography

N. Borderies and P. Goldreich. A simple derivation of capture probabilities for the J + 1 : J and J + 2 : J orbit-orbit resonance problems. *Celestial Mechanics*, 32:127-136, February 1984. *[This paper derives the probability of capture in mean motion resonance under slow variation of parameters.]*

B. V. Chirikov. A universal instability of many-dimensional oscillator systems. *Physics Reports*, 52:263–379, May 1979. *[This paper provides an introduction to the chaotic dynamics in systems with multiple frequencies.]*

J. M. A. Danby. *Fundamentals of celestial mechanics*. 1988. *[An excellent reference book for celestial mechanics.]*

K. A. Innanen, J.Q. Zheng, S. Mikkola, M.J. Valtonen. The Kozai Mechanism and the Stability of Planetary Orbits in Binary Star Systems. *Astron. J.*, 113:1915-1919, May 1997. *[This paper provides an excellent discussion of the Kozai-Lidov effect.]*

S. F. Dermott, R. Malhotra, and C. D. Murray. Dynamics of the Uranian and Saturnian satellite systems - A chaotic route to melting Miranda? *Icarus*, 76:295–334, November 1988. *[This paper describes mean motion resonance splittings, secondary resonances, resonance capture and chaotic escape from resonance in the Uranian satellite system.]*

B. Katz, S. Dong, and R. Malhotra. Long-Term Cycling of Kozai-Lidov Cycles: Extreme Eccentricities and Inclinations Excited by a Distant Eccentric Perturber. *Phys. Rev. Lett.*, 107:181101, 2011. *[A new analysis of octupole perturbations in the Kozai-Lidov effect.]*

M. Lecar, F.A. Franklin, M.J. Holman and N.J. Murray. Chaos in the Solar System. *Annual Reports of Astronomy & Astrophysics*, 39:581-631, 2001. *[A review of results on the chaotic orbital dynamics in the solar system.]*

J. J. Lissauer, D. Ragozzine, D. C. Fabrycky, J. H. Steffen, E. B. Ford, J. M. Jenkins, A. Shporer, M. J. Holman, J. F. Rowe, E. V. Quintana, N. M. Batalha, W. J. Borucki, S. T. Bryson, D. A. Caldwell, J. A. Carter, D. Ciardi, E. W. Dunham, J. J. Fortney, T. N. Gautier, III, S. B. Howell, D. G. Koch, D. W. Latham, G. W. Marcy, R. C. Morehead, and D. Sasselov. Architecture and Dynamics of Kepler's Candidate Multiple Transiting Planet Systems. *Astrophysical Journal–Supplement*, 197:8, November 2011. *[This paper describes recent discoveries of exo-solar multiple-planet systems discovered by the* Kepler *space telescope.]*

R. Malhotra, D. Black, A. Eck, and A. Jackson. Resonant orbital evolution in the putative planetary system of PSR1257 + 12. *Nature*, 356:583–585, April 1992. *[This paper shows that the pulsar-planet system is near an orbital resonance, and the resonant*

perturbations can be used to compute the planetary masses and orbital inclinations.]

R. Malhotra. The origin of Pluto's peculiar orbit. *Nature*, 365:819–821, 1993. *[This paper put forth the hypothesis that Pluto's orbital properties could be explained if Neptune and the other giant planets had migrated from their formation locations.]*

R. Malhotra, J. Williams. The heliocentric motion of Pluto, in Pluto and Charon, D.J. Tholen, S.A. Stern, eds., Arizona Space Science Series, Univ. of Arizona Press, Tucson (1997). *[A review of the dynamics of Pluto's orbit.]*

R. Malhotra and D.A. Minton. Prospects for the habitability of OGLE-2006-BLG-109L. *ApJ*, 683:L67, 2008. *[This paper uses secular resonance analysis to constrain the mass and orbit of a putative habitable zone planet in this exo-planet system discovered by means of microlensing observations.]*

D.A. Minton and R. Malhotra 2011. Secular Resonance Sweeping of the Main Asteroid Belt During Planet Migration. *ApJ* **732**, 53–+. *[This paper analyses the effects on the orbital eccentricities of asteroids due to secular resonance sweeping stemming from planet migration.]*

N. Murray and M. Holman. The Origin of Chaos in the Outer Solar System. *Science*, 283:1877–+, March 1999. *[This paper describes how higher oder, three-body resonances cause orbital chaos and instability.]*

S. J. Peale. Orbital resonances, unusual configurations and exotic rotation states among planetary satellites, pages 159–223. 1986. *[An excellent reference for orbital resonances and spin-orbit resonances found in planetary satellite systems.]*

A. P. Showman and R. Malhotra. The Galilean Satellites. *Science*, 296:77–84, October 1999. *[A review of the resonant orbital dynamics and physical properties of the classical Galilean moons of Jupiter.]*

W. C. Tittemore and J. Wisdom. Tidal evolution of the Uranian satellites. II - an explanation of the anomalously high orbital inclination of Miranda. *Icarus*, 78:63–89, March 1989. *[This paper describes mean motion resonance splittings, secondary resonances, resonance capture and chaotic escape from resonance in the Uranian satellite system.]*

W. R Ward, G Colombo, and F. A Franklin. Secular resonance, solar spin down, and the orbit of Mercury. *Icarus*, 28:441, 1976. *[This paper analyses effects on the orbit of planet Mercury due to secular resonance sweeping stemming from the dispersal of the solar nebula.]*

J. Wisdom. The resonance overlap criterion and the onset of stochastic behavior in the restricted three-body problem. *Astronomical Journal*, 85:1122–1133, August 1980. *[The first application of the resonance overlap criterion to derive the $\mu^{2/7}$ law for the size of the chaotic zone annulus around a planet's orbit.]*